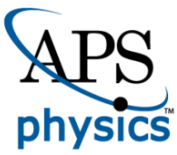

Enhancing network synchronization by phase modulation

Huawei Fan, Ying-Cheng Lai, and Xingang Wang

Phys. Rev. E **98**, 012212 — Published 20 July 2018

DOI: 10.1103/PhysRevE.98.012212

Enhancing network synchronization by phase modulation

Huawei Fan,[1] Ying-Cheng Lai,[1,2] Shi-Xian Qu,[1] and Xingang Wang[1,*]

[1]*School of Physics and Information Technology, Shaanxi Normal University, Xi'an 710062, China*
[2]*School of Electrical, Computer, and Energy Engineering, Arizona State University, Tempe, Arizona 85287, USA*

(Dated: June 25, 2018)

Due to time delays in signal transmission and processing, phase lags are inevitable in realistic complex oscillator networks. Conventional wisdom is that phase lags are detrimental to network synchronization. Here we show that judiciously chosen phase lag modulations can result in significantly enhanced network synchronization. We justify our strategy of phase modulation, demonstrate its power in facilitating and enhancing network synchronization with synthetic and empirical network models, and provide an analytic understanding of the underlying mechanism. Our work provides a new approach to synchronization optimization in complex networks, with insights into control of complex nonlinear networks.

I. INTRODUCTION

The function and operation of realistic complex systems rely on the coherent motion of their constituent dynamical elements, generating a continuous interest in the synchronization behaviors of coupled oscillators [1–5]. In the study of oscillator synchronization, an issue of theoretical and practical significance is how to achieve global synchronization in a large-scale networked system at reduced coupling cost [3–5]. In the past, a number of strategies were proposed and studied to address the problem of synchronization optimization in coupled oscillator networks systems [6–11]. For example, the small-world and scale-free features in engineering and natural systems [12, 13] have been exploited to achieve optimal synchronization in complex networks [14–19].

A paradigm in the study of network synchronization is the Kuramoto model [1], in which an ensemble of phase oscillators with distributed natural frequencies are coupled in a nonlinear fashion and can be locked in phase when the mutual coupling parameter exceeds a critical value. The Kuramoto model and its generalized forms capture the essence of the collective dynamics of many realistic systems [20–23], and have been exploited as a standard model for testifying the efficiency of various synchronization optimization strategies [11, 12, 15–19, 24–29]. In terms of optimization, the existing synchronization strategies can be classified into two major categories: one based on adjusting the network structure and another seeking/arranging optimal locations for oscillators. Strategies based on network structural perturbations are applicable to situations where the nodal dynamics are fixed but there is flexibility in modifying the link structure such as the addition of shortcuts [12, 15]. The alternative strategy applies to situations where the network structure cannot be altered but it is possible to rearrange the locations of the oscillators according to the network structure [11, 18, 25]. There have been theoretical efforts in establishing the efficiency of the various synchronization optimization strategies. However, to physically realize certain strategies, e.g., to supply shortcut links in a real neuronal network or to relocate a pair of power stations in an actual power grid, may be difficult. It remains to be an open and challenging problem to articulate physically reasonable strategies to optimize synchronization in complex networks of coupled nonlinear oscillators.

Due to the limited speed of signal transmission and processing, time delay is ubiquitous in real world systems. For a network of coupled oscillators, a time delay represents a phase lag in the interaction. In previous studies, time delays are generally considered as detrimental to synchronization [26, 27, 30–36]. When a uniform phase lag exists in the coupling, global synchronization can be destroyed, leading to the emergence of alternative types of collective dynamics on the network. For example, when the value of the phase lag is about $\pi/2$, a chimera state [34, 35] can arise, in which both synchronized and unsynchronized groups of oscillators coexist. For π phase lag, anti-phase synchronization clusters can form [37, 38]. For random phase lags, the onset of synchronization can be significantly delayed or even disappear [31, 32]. Motivated by the ubiquity of time delay and its strong ability to alter the network synchronization dynamics, we ask the following question of both basic and practical significance: is it possible to exploit phase lag modulations for synchronization optimization? More specifically, we ask whether it would be possible to apply judiciously chosen phase lags to enhance network synchronization, as in applications where synchronous dynamics are desired. The main contribution of this paper is an affirmative answer to this question.

In general, the amount of phase lag for an oscillator will depend on the its intrinsic dynamics or state, and the phase lags cannot be expected to be uniform among the oscillators in the network. An advantage of this approach is that phase modulation does not require the adjustment of the network structure or relocation of the oscillators. Our phase modulation based strategy thus holds the promise of achieving optimal, highly efficient synchronization in complex oscillator networks at low cost. More specifically, we consider complex networks of coupled phase oscillators with fixed network structure and oscillator arrangement. We introduce to each oscillator a constant phase lag whose amount is determined by the natural frequency of the oscillator. We demonstrate numerically and argue analytically that the proposed phase mod-

* Email address:wangxg@snnu.edu.cn

ulation scheme is capable of dramatically improving network synchronization, as characterized by a marked increase in the value of the synchronization order parameter and a significant decrease in the critical coupling strength for global synchronization. The phase modulation strategy is physically realizable and practically implementable, opening a new approach to investigating optimization and control of collective dynamics in complex nonlinear networks.

In Sec. II, we describe networked systems of coupled phase oscillators, introduce the phase-modulation strategy, and provide numerical results on the effect of phase modulation on synchronization. In Sec. III, we present a theoretical analysis to explain the underlying mechanism enhancing synchronization. In Sec. IV, we apply our phase modulation strategy to two empirical systems: the neuronal network of nematode C. Elegans and a power grid network. In Sec. V, we present results of optimizing synchronization using a partial phase modulation scheme and compare the performance of the phase-modulation strategy to that of two recent optimization approaches. In Sec. VI, we summarize and present a discussion of the main result.

II. MODEL AND PHENOMENA

Our model of networked phase oscillators reads

$$\dot{\theta}_i = \omega_i + \frac{K}{d_i}\sum_{j=1}^{N} a_{ij}\sin(\theta_j - \theta_i - \alpha_i), \tag{1}$$

where $i, j = 1, \ldots, N$ are the oscillator (node) indices, $\theta_i(t)$ is the instant phase of the ith oscillator at time t, and K is the uniform coupling strength. The natural frequency of the ith oscillator is ω_i, which follows the distribution $g(\omega)$. The coupling relationship of the oscillators is described by the adjacency matrix $A = \{a_{ij}\}$, with $a_{ij} = a_{ji} = 1$ if oscillators i and j are directly coupled by a link, otherwise $a_{ij} = 0$. The quantity $d_i = \sum_j a_{ij}$ is the number of connections associated to oscillator i, i.e., its degree, and α_i is the phase modulation introduced to oscillator i, which depends on ω_i (with a specific form given below). Equation (1) is similar in form to the generalized Kuramoto-Sakaguchi model, which has been extensively studied in the literature for various synchronization phenomena among networked oscillators [30–35, 37, 38].

Different from existing models where α_i is uniform or randomly distributed, we judiciously set α_i based on the information of the oscillator dynamics. The specific form of α_i and the reason behind are the following. For an ensemble of coupled phase oscillators whose natural frequencies follow a given distribution, the occurrence of synchronization is determined by two counter-balancing factors: coupling and frequency spread [20–22]. Whereas the former tends to make the oscillators coherent, the latter prevents this tendency. In the presence of coupling, the effective frequency of each oscillator is different from its natural frequency. As the coupling strength is increased from zero, the spread of the effective frequencies will be gradually narrowed. At the critical point of global synchronization, the effective frequencies of the oscillators become identical, giving rise to the synchronous motion. This intuitive picture gives an important indication on how to enhance synchronization by modulating phase lags in Eq. (1): narrowing the distribution of the effective frequencies of the oscillators by tuning α_i.

Assume that the system is in the vicinity of the global synchronization state: $\theta_i(t) \approx \theta_j(t)$ for $i, j = 1, \ldots, N$. Equation (1) can be approximated as

$$\dot{\theta}_i = \tilde{\omega}_i + \frac{K}{d_i}\sum_{j=1}^{N} a_{ij}(\theta_j - \theta_i)\cos(\alpha_i), \tag{2}$$

where $\tilde{\omega}_i = \omega_i - K\sin\alpha_i$ is the modified natural frequency of oscillator i. Requiring $\tilde{\omega}_i = 0$, we have $\omega_i - K\sin\alpha_i = 0$, which gives $\alpha_i = \arcsin(\omega_i/K)$. Setting phase lags this way, the modified natural frequencies of all the oscillators will be identical, facilitating synchronization. To keep $\tilde{\omega}_i = 0$ for all the oscillators, it is necessary that $K \geq K_c \equiv \omega_{max}$ be satisfied, with $\omega_{max} = \max\{|\omega_i|\}$ being the largest natural frequency of the oscillators. To make α_i independent of K (so that α_i is a constant value for each oscillator), we introduce the phase modulation scheme

$$\alpha_i = \arcsin(\beta\omega_i), \tag{3}$$

with $\beta \in [0, \beta_{max}]$ being the modulation amplitude. Here the quantity $\beta_{max} = 1/K_c = 1/\omega_{max}$ is the largest modulation amplitude capable of generating identical effective frequency. With Eq. (3), the modified natural frequencies can be rewritten as $\tilde{\omega}_i = \omega_i(1 - K\beta)$.

The effects of phase modulation on synchronization can be intuitively understood, as follows. For a fixed value of β, as K is increased from zero, the distribution of $\tilde{\omega}_i$ will be gradually narrowed, resulting in enhanced synchronization. At the critical point $K_c^\beta = 1/\beta$, we have $\tilde{\omega}_i = 0$ for all oscillators, signifying that global synchronization has been achieved. For $K > K_c^\beta$, $\tilde{\omega}_i$ spreads out again, deteriorating synchronization. As β is increased from zero to β_{max}, the critical coupling strength K_c^β will decrease gradually. For $\beta = \beta_{max}$, we get the minimum critical coupling strength for global synchronization: $K_c = 1/\beta_{max} = \omega_{max}$.

To test the proposed phase modulation scheme, we carry out simulations using a variety of network models. In all cases, the size of the network is $N = 200$ and the natural frequencies of the oscillators follow the truncated Lorentzian distribution: $g(\omega) = (\delta/\pi)/[(\omega - \omega_0)^2 + \delta^2]$. The central frequency, scale parameter and truncation frequency of the Lorentzian distribution are $\omega_0 = 0$, $\delta = 1$, and $\omega_{max} = 2.0$, respectively. Network synchronization is characterized by the order parameter

$$R = \langle | \sum_{j=1}^{N} e^{i\theta_j} | \rangle$$

where $|\cdot|$ and $\langle\cdot\rangle$ denote, respectively, the module and time averaged functions, and $R \in [0, 1]$, with $R = 0$ and 1 corresponding to completely incoherent and global synchronization states, respectively. Figures 1(a-d) show, for globally

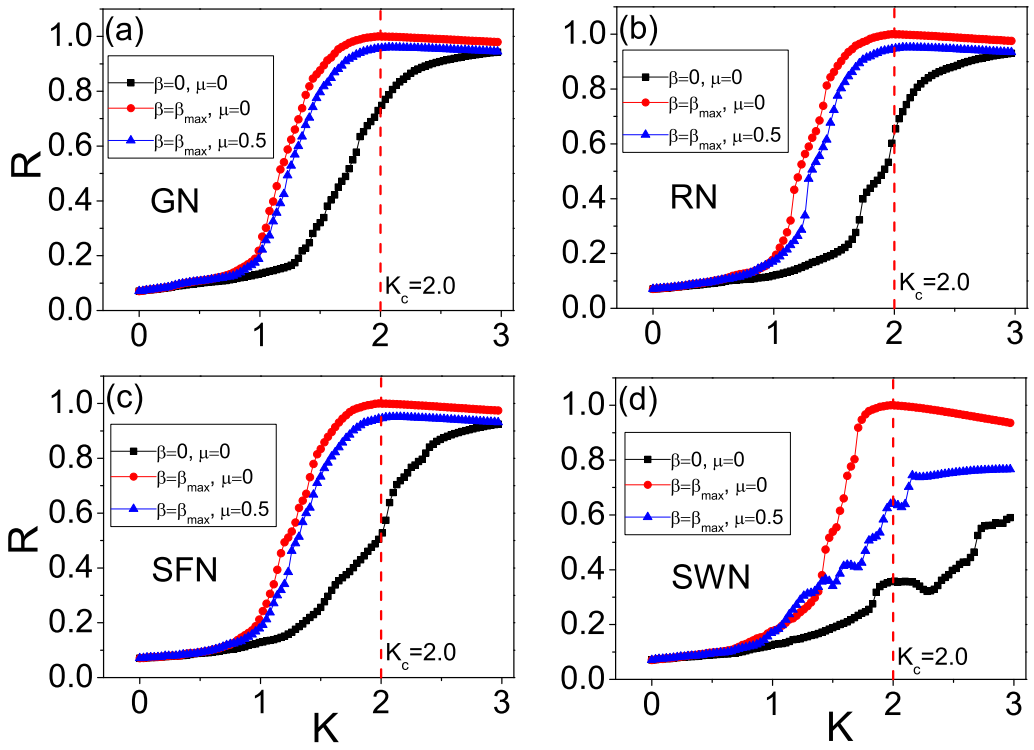

FIG. 1. (Color online) The impact of phase modulation on synchronization in different network models. (a-d) For globally connected (GN), random (RN), scale-free (SFN), and small-world (SWN) networks, the order parameter R versus the coupling strength K with or without phase modulation and noise perturbations: $(\beta, \mu) = (0, 0)$ (black squares), $(\beta, \mu) = (\beta_{max}, \mu) = (0.5, 0)$ (red circles), $(\beta, \mu) = (0.5, 0.5)$ (blue triangles). The network size is $N = 200$. The average degree of the networks in (b-d) is $\langle k \rangle = 16$. The rewiring probability for the small-world networks is 0.1. In all network models, the critical value of the coupling parameter is $K_c = 1/\beta_{max} = \omega_{max} = 2.0$, which agrees with the theoretical prediction. Each data point is the result of averaging over 20 statistical realizations.

connected, random [39], scale-free [13], and small-world networks [12], respectively, the order parameter R versus the coupling parameter K for different values of the modulation amplitude β. We see that, when phase modulation is applied, the values of the order parameters are consistently larger than those without phase modulation, and transition to global synchronization characterized by $R = 1$ occurs for much smaller value of K. It is noted that, with phase modulation, the critical value of the coupling parameter at which R reaches unity is $K_c = \omega_{max} = 2.0$, regardless of the network structure. (This property is rooted in the normalized coupling strategy we have adopted in the model.) As K is increased further, the value of R tends to reduce slightly.

To assess the robustness of the phase modulation strategy in facilitating and enhancing network synchronization, we perturb the phase lags by introducing independent and identically distributed random noise: $\alpha_i = \alpha_{0i} + \mu W_i$, where α_{0i} is the phase lag given by Eq. (3), W_i is a random number uniformly distributed in the interval $[-1, 1]$, and μ is the noise amplitude. Figure 1 shows that, while random noise tends to reduce the value of the order parameter and thus weaken synchronization, the negative effect on synchronization is insignificant, suggesting the robustness of the phase-modulation-based strategy to noise perturbations.

To gain further insights into the role of phase modulation in network synchronization, we examine the variations of the effective frequencies, $\omega_i^{eff} = (1/T) \int_t^{t+T} \dot{\theta}_i(\tau) d\tau$, with respect to K, where $\dot{\theta}_i(\tau)$ stands for the instantaneous frequency of oscillator i. Figure 2(a) shows the numerical results for the model of globally connected network. We see that, as K is increased from zero, the distribution of the effective frequencies is gradually narrowed. As the critical coupling strength K_c is reached, all effective frequencies converge to a single value. Figure 2(b) shows the variations of the phase difference, $\Delta\theta_i = \theta_i - \psi$, where ψ is the average phase defined by the relation $e^{i\psi} = \sum_j e^{i\theta_j}/R$. We see that the phase differences are random for $K < K_c$, become zero at K_c, and exhibit a systematic delayed behavior as K is increased through K_c. This phenomenon is consistent with the numerical results in Fig. 1, where R exhibits a slightly decreasing trend as the value of K is increased through K_c. For models other than the globally connected network, we obtain essentially the same results.

The results in Figs. 1 and 2 reveal the following physical picture about the transition to synchronization in the presence of phase modulation. As the value of K is increased from zero, the difference between the modulated natural frequencies [i.e., $\tilde{\omega}_i$ in Eq. (3)] gradually decreases, resulting in

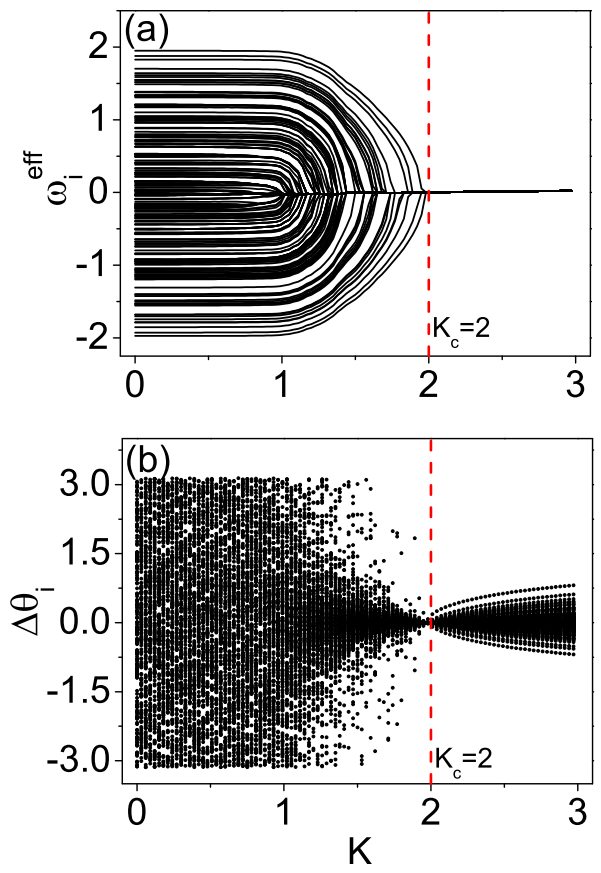

FIG. 2. Behaviors of frequency and phase in the presence of phase modulation. For the model of globally connected network in Fig. 1(a), the distribution of (a) the effective frequency ω_i^{eff} and (b) the phase difference $\Delta\theta$ taken at $t = 1 \times 10^3$ versus the coupling strength K. In (a), all the effective frequencies converge to zero for $K \geq K_c$. In (b), the phase differences first converge for $K < K_c$ and then diverge for $K > K_c$. At the critical point $K = K_c$, all the phase differences vanish.

the convergence of the effective frequencies [Fig. 2(a)] and an increase in the value of the order parameter [Fig. 1]. At $K = K_c$, we have $\tilde{\omega}_i = 0$ for all the oscillators and, due to the strong coupling strength, the phases of the oscillators are nearly identical, leading to the highest level of synchronization ($R \approx 1$). As the value of K is increased from K_c, $\tilde{\omega}_i$ become non-identical again. However, since the value of K is large, the oscillators are still locked in frequency [Fig. 2(a)] but with scattered phases [Fig. 2(b)]. It is the scattered phases which lead to the decrease of R in the parameter region $K > K_c$ [Fig. 1].

III. THEORETICAL ANALYSIS

We use the Ott-Antonsen ansatz [16] to obtain an analytic understanding of the mechanism underlying phase-modulation enhanced synchronization. For the model of globally connected network [Figs. 1(a) and 2], the dynamics of the phase oscillators can be rewritten as

$$\dot{\theta}_i = \omega_i + [K/(2i)][(re^{-i\theta_i} - cc)\cos\alpha_i - i(re^{-i\theta_i} + cc)\sin\alpha_i], \quad (4)$$

where cc stands for the complex conjugate and $r = Re^{i\psi}$. In the thermodynamic limit $N \to \infty$, the state of the system at time t can be described by a probability density function $f[\omega(\alpha), \theta, t] \equiv f(\omega, \theta, t)$, whose evolution is governed by the continuity equation

$$\partial f/\partial t + \partial\{[\omega + \frac{K}{2i}(re^{-i\theta_i} - c.c.)h_2(\omega) - \frac{K}{2}(re^{-i\theta_i} + c.c.)h_1(\omega)]f\}/\partial\theta = 0, \quad (5)$$

where $h_2(\omega) = \sqrt{1-\beta^2\omega^2} = \cos\alpha \in (0,1)$ and $h_1(\omega) = \beta\omega = \sin\alpha \in (-1,1)$. The complex order parameter can be expressed as $r = \int_0^{2\pi} d\theta \int_\infty^\infty d\omega f(\omega,\theta,t)e^{i\theta}$.

Expanding $f(\omega,\theta,t)$ as a Fourier series in θ, we have

$$f = \frac{g(\omega)}{2\pi}[1 + \sum_{n=1}^{\infty} f_n(\omega,t)e^{in\theta} + \sum_{n=-\infty}^{-1} f_n^*(\omega,t)e^{in\theta}]. \quad (6)$$

Utilizing the Ott-Antonsen ansatz [16]: $f_n(\omega,t) = a(\omega,t)^n$, for $|a(\omega,t)| \leq 1$, we obtain

$$\frac{\partial a}{\partial t} + i\omega a + \frac{K}{2}(ra^2 - r^*)h_2(\omega) - \frac{K}{2}(ira^2 + ir^*)h_1(\omega) = 0 \quad (7)$$

and

$$r^* = \int_{-\infty}^{\infty} d\omega a(\omega,t)g(\omega). \quad (8)$$

We use the Lorentzian distribution for the natural frequencies: $g(\omega) = 1/(i2\pi)[(\omega - \omega_0 - i\delta)^{-1} - (\omega - \omega_0 + i\delta)^{-1}]$. To evaluate the integral that gives r^*, we analytically continue ω to the complex ω-plane and carry out contour integration [16], where the analyticity of α holds in the lower half plane of the complex variable ω. For large negative values of $\mathrm{Im}(\omega)$, Eq. (7) can be approximated as $\partial a/\partial t = \mathrm{Im}(\omega)a$, so we have $a \to 0$ for $\mathrm{Im}(\omega) \to -\infty$. Following the setting of numerical simulations, we have $\omega_0 = 0$ and $\delta = 1$ for the Lorentzian distribution. The pole of the lower half plane is $\omega = -i$. We thus obtain $r = a^*(-i,t)$. Substituting this expression into Eq. (7), we get the following nonlinear equation for the order parameter

$$\frac{\partial R}{\partial t} + [1 - \frac{K}{2}(\sqrt{1+\beta^2}+\beta)]R + \frac{K}{2}(\sqrt{1+\beta^2}-\beta)R^3 = 0, \quad (9)$$

which is the Bernoulli equation with a proper solution given by

$$\frac{R(t)}{R_0} = \{1 + (\frac{R_0^2}{R(0)^2} - 1)e^{2t[1-\frac{K}{2}(\sqrt{1+\beta^2}+\beta)]}\}^{-1/2}, \quad (10)$$

where

$$R_0 = |\frac{\sqrt{1+\beta^2}-\beta}{\sqrt{1+\beta^2}+\beta-\frac{2}{K}}|^{-\frac{1}{2}}.$$

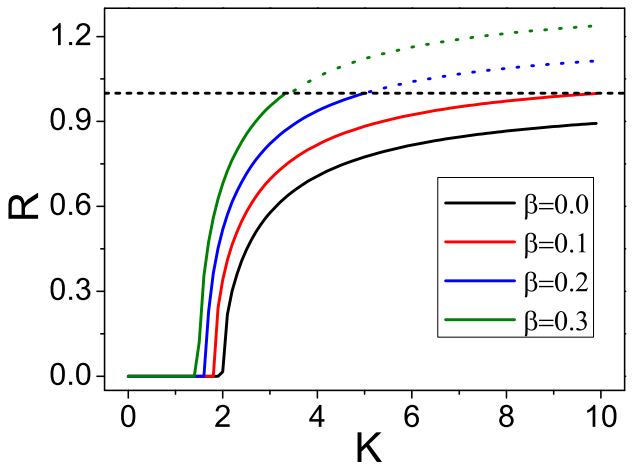

FIG. 3. (Color online) Theoretically predicted values of the order parameter in the presence of phase modulation. For the model of globally connected network, the order parameter R calculated from the analytic prediction Eq. (10) versus the coupling parameter K for different amplitudes of phase modulation: $\beta = 0$ (black), $\beta = 0.1$ (red), $\beta = 0.2$ (blue), and $\beta = 0.3$ (green). With phase modulation, R reaches unity at a finite value of the coupling strength: $K_c = 1/\beta$. However, without phase modulation, this occurs for $K_c \to \infty$ (black).

We see that for $K < K_0 = 2/(\sqrt{1+\beta^2}+\beta)$, $R(t)$ tends to zero exponentially with time. For $K > K_0$, $R(t)$ approaches asymptotically a finite value R_0, where K_0 is the critical coupling at which the value of R begins to increase from zero, i.e., onset of synchronization [17, 19]. Setting $R_0 = 1$, we can obtain the critical coupling strength for global synchronization as $K_c^\beta = 1/\beta$, which agrees with the heuristic argument in Sec. II.

Figure 3 shows the theoretically predicted value of R from Eq. (10) versus K for different values of β. We observe two features. Firstly, prior to the onset of global synchronization ($K < K_c$), the value of the order parameter R increases monotonically with β. Secondly, as the value of β is increased from zero, the critical coupling strength for global synchronization gradually decreases. Specifically, Eq. (10) predicts that, without phase modulation ($\beta = 0$), the onset of global synchronization occurs at infinite coupling strength ($K_c \to \infty$), whereas with phase modulation, this happens at a finite value: $K_c = 1/\beta$. The theoretical prediction agrees well with the numerical results in Figs. 1 and 2.

While Eq. (10) predicts that the R values can be greater than unity, they are not physically meaningful. As depicted in Fig. 2(b), once K exceeds the critical value K_c, phase lags among the oscillators will set in, causing R to decrease from unity. The seeming contradiction between the theoretical and numerical results for $K > K_c$ can be explained, as follows. Substituting $a = |a|e^{i\varphi}$ into Eq. (7), we get

$$\partial|a|/\partial t + (K/2)(|a|^2-1)\mathrm{Re}(re^{-i\varphi})h_2(\omega) + (K/2)(|a|^2+1)\mathrm{Im}(re^{-i\varphi})h_1(\omega) = 0, \quad (11)$$

which indicates that, quite different from the case without phase modulation [16], $\partial|a|/\partial t \neq 0$ for $|a| = 1$. This means that a trajectory of Eq. (7) originated from some initial condition satisfying $|a| < 1$ may cross the unit circle in the complex a-plane. Since $r = a^*(-i,t)$, the situation of $R > 1$ can occur. In fact, for $|a| > 1$, the Ott-Antonsen ansatz is no longer valid [16], making the analytic prediction for this regime physically meaningless.

IV. APPLICATIONS

We demonstrate the enhancement of synchronization by the strategy of phase modulation in two realistic systems. The first example is the neuronal network of the nematode C. Elegans [40], in which phase lags in coupling interaction can be modulated using methods such as drug delivery [41]. The structure of the neuronal network is shown in Fig. 4(a), which consists of $N = 297$ nodes and 2148 links. Following Refs. [42, 43], we represent the dynamics of isolated neurons by non-identical phase oscillators and investigate their collective behavior using the generalized Kuramoto model Eq. (1). We adopt the Lorentzian distribution for the natural frequencies and set $\alpha_i = \arcsin(\beta\omega_i)$. The numerical results with and without phase modulation are presented in Fig. 4(b). We see that phase modulation can dramatically facilitate synchronization. Particularly, without phase modulation, global synchronization occurs at $K_c \approx 8$, whereas with phase modulation, this occurs at $K_c = 1/\beta \approx 3.3$.

The second example is the RTS-96 power grid, whose structure is shown in Fig. 4(c), which has $N = 73$ nodes and 214 links. To be realistic, we divide the nodes into two groups, generators and loads, and model their dynamics by the generic swing equations [44, 45]:

$$M_i\ddot{\theta}_i + D_i\dot{\theta}_i = \omega_i + \frac{K}{d_i}\sum_{j=1}^{N} a_{ij}\sin(\theta_j - \theta_i - \alpha_i),\ i \in V_1,$$
$$D_l\dot{\theta}_l = \omega_l + \frac{K}{d_l}\sum_{j=1}^{N} a_{lj}\sin(\theta_j - \theta_l - \alpha_l),\ l \in V_2, \quad (12)$$

where V_1 and V_2 denote the sets of generator and load nodes, respectively, M_i is the inertial coefficient for generator node i, and D_i is the viscous damping coefficient. Adopting the Lorentzian frequency distribution and setting $\alpha_i = \arcsin(\beta\omega_i)$, we obtain the variation of R versus K with and without phase modulation, as shown in Fig. 4(d). (In simulations, we increase K adiabatically from zero so as to avoid the problem of multiple coexisting attractors [46].) We see that, with phase modulation, synchronization is both facilitated and enhanced. In particular, without phase modulation, global synchronization is not reached even for $K = 16$, whereas even with weak phase modulation ($\beta = 0.1$), global synchronization occurs at $K_c \approx 10$. For a realistic power grid, phase modulation can be realized by adjusting the power angles between the exciting and terminal voltages [47].

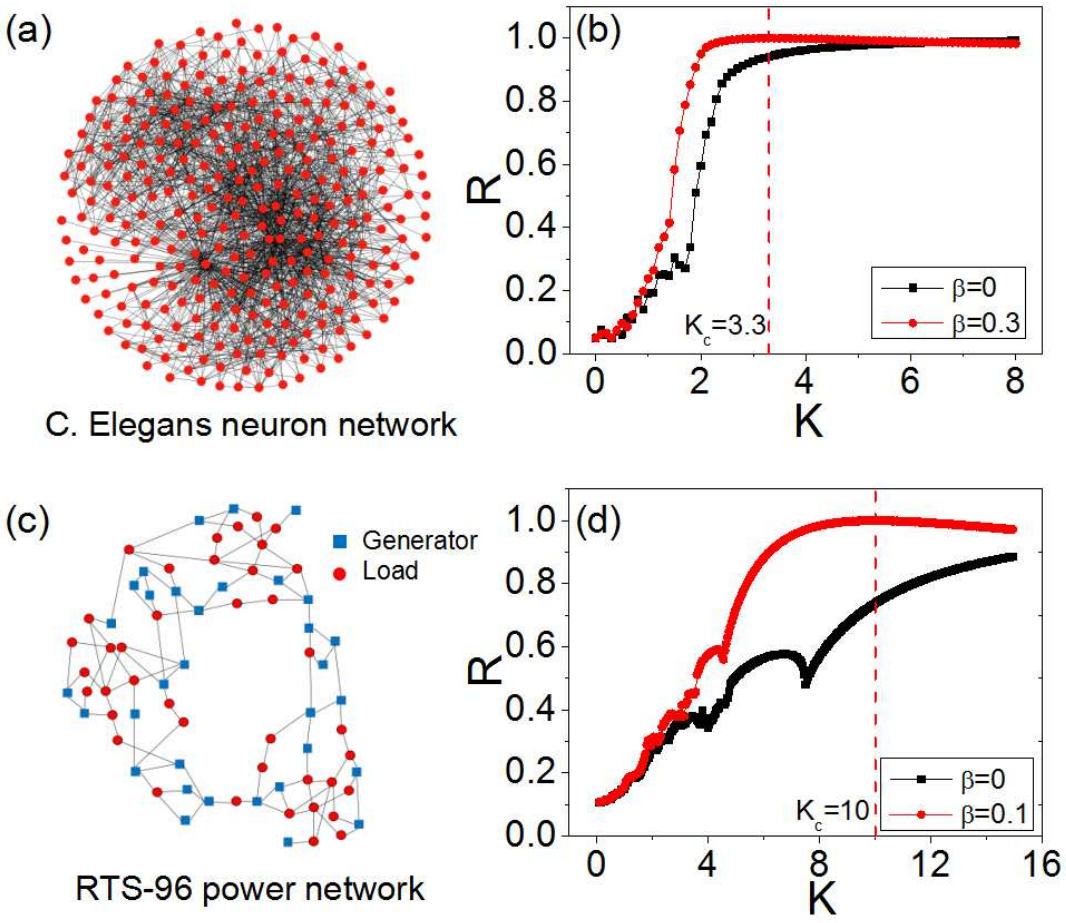

FIG. 4. (Color online) Synchronization optimization by phase modulation in realistic networks. (a) The structure of the neuronal network of the nematode C. Elegans. (b) For the neuronal network, R versus K when phase modulation is absent ($\beta = 0$, black squares) and present ($\beta = 0.3$, red circles). (c) The structure of the RTS-96 power grid. Blue squares and red nodes denote, respectively, generators and loads. (d) For the power-grid network, the variation of synchronization order parameter, R, with respect to the coupling strength, K, for the cases where phase modulation is absent ($\beta = 0$, black squares) and present ($\beta = 0.1$, red circles). For both networks, the natural frequency of the nodes follows the Lorentz distribution, with the truncation frequency $\max\{|\omega|\} = 2.0$, the location parameter $\omega_0 = 0$ and the scale parameter $\delta = 1$. Results in (b) and (d) are averaged over 20 frequency realizations.

V. PARTIAL PHASE MODULATION SCHEME AND COMPARISON WITH TWO RECENT OPTIMIZATION APPROACHES

Our study has focused on the case where phase modulation is introduced to each oscillator in the network, this is not necessary in practical applications. In fact, network synchronization can still be significantly enhanced if phase modulation is introduced to only a fraction of the oscillators. To demonstrate this, we use the globally connected network in Fig. 1(a) and introduce phase modulation to only $p = 20\%$ of the oscillators, with the targeting oscillators selected in a descending order of the oscillator natural frequency. The numerical results are presented in Fig. 4(a). We see that, comparing with the case without phase modulation, synchronization with partial phase modulation is significantly enhanced. As the fraction p of modulated oscillators is increased, the synchronization performance approaches that with global phase modulation - the upper limit.

Our work is related to but distinct from two recent studies: explosive synchronization [18] and J-function-based synchronization optimization [11]. In explosive synchronization, it is the counter-balance between heterogeneous network structure and non-identical nodal dynamics which results in a first-order transition to synchronization [22], whereas in our present work heterogeneity in the nodal dynamics is balanced by phase lags. Different from explosive synchronization, our phase modulation strategy does not require any resetting of the oscillator frequencies and, in terms of synchronization optimization, outperforms the frequency-weighted strategy adopted in explosive synchronization. For instance, for the model of globally connected network (with the same coupling scheme and frequency distribution used in our present work), the critical forward coupling strength in explosive synchronization is always larger than [28] $K_c = 2.0$, while through phase modulation the critical coupling strength for

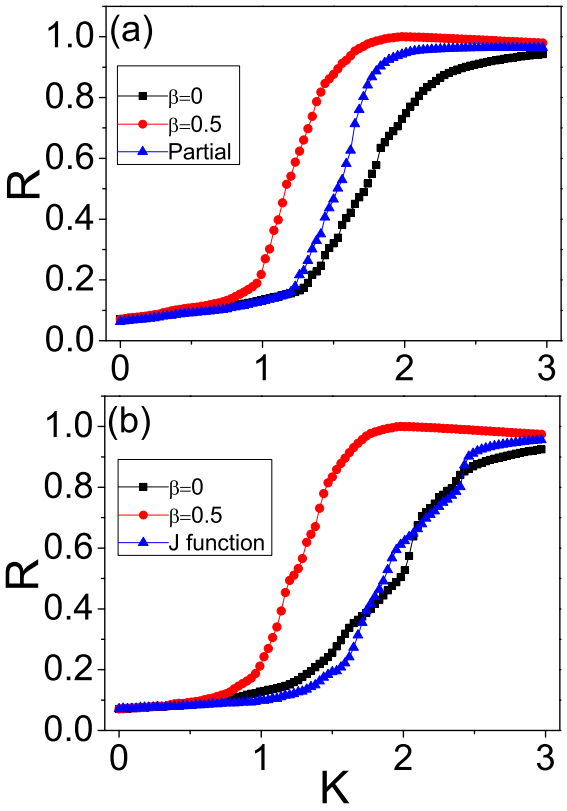

FIG. 5. (Color online) Effect of partial phase modulation. (a) For the model of globally connected network in Fig. 1(a), order parameter R versus the coupling strength K for partial phase modulation (blue triangles) in which phase lags are introduced to only $p = 10\%$ of the oscillators. (b) For the model of scale-free network in Fig. 1(b), R versus K for phase modulation and J-function based synchronization strategies. In both panels, the results without ($\beta = 0$, black squares) and with global ($\beta = 0.5$, red circles) phase modulation are also included for comparison.

global synchronization is universally $K_c = 2.0$ for all network models [Fig. 1]. The J-function method, on the other hand, is a synchronization-optimization-oriented function [11] aiming to improve synchronization in complex network of coupled phase oscillators. The J-function, which combines the information of network structure (i.e., the eigenvectors of the network coupling matrix) and oscillator dynamics (e.g., the natural frequencies of the oscillator), provides an efficient numerical approach to finding the optimal configuration of oscillators in large networks. Using the model of scale-free network in Fig. 1(c), we compare the synchronization performance of the J-function-based and phase-modulation-based strategies. (In searching for the optimal configuration, we iterate the J-function 1×10^6 times, following the method proposed in Ref. [11]. To make the comparison on an equal footing, we adopt the same ensemble of natural frequencies for the oscillators.) The results are presented in Fig. 4. We see that the performance of the J-function-based strategy is lower than that of phase-modulation-based strategy. As the scheme of normalized coupling strength is concerned [Eq. (2)], the optimal configuration has almost the same synchronization performance as that of random configuration, as shown in Fig. 4(b).

VI. DISCUSSION

To summarize, we have proposed a phase-modulation based strategy for facilitating and enhancing synchronization in complex networks and demonstrated its efficiency using a variety of network models as well as two realistic networks. The strategy should be distinguished from the existing methods of synchronization optimization in that it does not require any adjustment of the network structure or the locations of the oscillators. More importantly, our work demonstrates that time delays, in contrast to conventional wisdom that they are detrimental to synchronization, can actually benefit synchronization. As time delays are ubiquitous in natural systems and phase lags can be implemented in practice, our strategy is physically realizable for realistic complex systems such as infrastructure and biological networks. Our study provides a novel approach to optimizing synchronization in complex networks of coupled nonlinear oscillators, with potential applications in the design of low cost, highly efficient synchronization solutions. The finding that synchronization can be improved by partial phase modulation provides useful insights into the control of dynamics in complex nonlinear systems - a challenging problem in nonlinear science and complex systems at present.

That synchronization performance can be improved by introducing phase lags to a fraction of all oscillators has implications to the problem of controlling complex nonlinear networks. In an early study, phase modulation was proposed for harnessing chaos in low-dimensional nonlinear systems, e.g., the chaotic Duffing oscillator [48]. What we have achieved here is to extend the idea of phase control to optimizing synchronization in complex spatiotemporal systems consisting of an ensemble of oscillators. As phase lags are ubiquitous and can be modulated in realistic systems, we hope that the strategy will find applications in controlling and optimizing complex infrastructure and biological systems, e.g., the power grid and neuronal networks.

ACKNOWLEDGEMENT

This work was supported by the National Natural Science Foundation of China under the Grant No. 11375109 and by the Fundamental Research Funds for the Central Universities under the Grant Nos. GK201601001 and 2017TS003. YCL was supported by ONR through Grant No. N00014-16-1-2828.

[1] Y. Kuramoto, *Chemical Oscillations, Waves, and Turbulence* (Springer, Berlin, 1984).

[2] A. Pikovsky, M. Rosenblum, and J. Kurths, *Synchronization: A Universal Concept in Nonlinear Science* (Cambridge Univer-

sity Press, Cambridge, 2003).
[3] S. Boccaletti, V. Latora, Y. Moreno, M. Chavez, and D.-U. Hwang, Complex networks: Structure and dynamics, Phys. Rep. **424**, 175 (2006).
[4] S. N. Dorogovtsev, A. V. Goltsev, and J. F. F. Mendes, Critical phenomena in complex networks, Rev. Mod. Phys. **80**, 1275 (2008).
[5] A. Arenas, A. Díaz-Guilera, J. Kurths, Y. Moreno, and C. S. Zhou, Synchronization in complex networks, Phys. Rep. **469**, 93 (2008).
[6] A. E. Motter, C. S. Zhou, and J. Kurths, Enhancing complex-network synchronization, EPL **69**, 334 (2005).
[7] T. Nishikawa and A. E. Motter, Synchronization is optimal in nondiagonalizable networks, Phys. Rev. E **73**, 065106 (2006).
[8] X. G. Wang, Y.-C. Lai, and C. H. Lai, Enhancing synchronization based on complex gradient networks, Phys. Rev. E **75**, 056205 (2007).
[9] L. Huang, Y.-C. Lai, and R. A. Gatenby, Optimization of synchronization in complex clustered networks, CHAOS **18**, 013101 (2008).
[10] A. Zeng, S. W. Son, C. H. Yeung, Y. Fan, and Z. R. Di, Enhancing synchronization by directionality in complex networks, Phys. Rev. E **83**, 045101 (2011).
[11] P. S. Skardal, D. Taylor, and J. Sun, Optimal synchronization of complex networks, Phys. Rev. Lett. **113**, 144101 (2014).
[12] D. J. Watts and S. H. Strogatz, Collective dynamics of 'small-world' networks, Nature **393**, 440 (1998).
[13] A.-L. Barabási and R. Albert, Emergence of scaling in random networks, Science **286**, 509 (1999).
[14] M. Barahona and L. M. Pecora, Synchronization in small-world systems, Phys. Rev. Lett. **89**, 054101 (2002).
[15] Y. Moreno and A. F. Pacheco, Synchronization of Kuramoto oscillators in scale-free networks, EPL **68**, 603 (2004).
[16] E. Ott and T. M. Antonsen, Low dimensional behavior of large systems of globally coupled oscillators, CHAOS **18**, 037113 (2008).
[17] X. G. Wang, L. Huang, S. Guan, Y.-C. Lai, and C.-H. Lai, Onset of synchronization in complex gradient networks, CHAOS 18, 037117 (2008)
[18] J. Gomez-Gardenes, S. Gomez, A. Arenas, and Y. Moreno, Explosive synchronization transitions in scale-free networks, Phys. Rev. Lett. **106**, 128701 (2011).
[19] M. Li, X. G. Wang, Y. Fan, Z. Di, and C.-H. Lai, Onset of synchronization in weighted complex networks: The effect of weight-degree correlation, CHAOS **21**, 025108 (2011).
[20] J. A. Acebron, L. L. Bonilla, C. J. P. Vicente, F. Ritort, and R. Spigler, The Kuramoto model: A simple paradigm for synchronization phenomena, Rev. Mod. Phys. **77**, 137 (2005).
[21] F. A. Rodrigues, T. K. D. M. Peron, P. Ji, and J. Kurths, The Kuramoto model in complex networks, Phys. Rep. **610**, 1 (2016).
[22] S. Boccaletti, J. A. Almendral, S. Guan, I. Leyva, Z. Liu, I. Sendina-Nadal, Z. Wang, and Y. Zou, Explosive transitions in complex networks' structure and dynamics: Percolation and synchronization. Phys. Rep. **660**, 1 (2016).
[23] S. Watanabe and S. H. Strogatz, Integrability of a globally coupled oscillator array, Phys. Rev. Lett. **70**, 2391 (1993).
[24] Z. Zheng, G. Hu, and B. Hu, Phase slips and phase synchronization of coupled oscillators, Phys. Rev. Lett. **81**, 5318 (1998).
[25] Y. Wu, J. Xiao, G. Hu, and M. Zhan, Synchronizing large number of nonidentical oscillators with small coupling, EPL **97**, 40005 (2012).
[26] O. E. Omelchenko and M. Wolfrum, Nonuniversal transitions to synchrony in the Sakaguchi-Kuramoto model, Phys. Rev. Lett. **109**, 164101 (2012).
[27] D. Iatsenko, S. Petkoski, P. V. E. McClintock, and A. Stefanovska, Stationary and traveling wave states of the Kuramoto model with an arbitrary distribution of frequencies and coupling strengths, Phys. Rev. Lett. **110**, 064101 (2013).
[28] X. Zhang, X. Hu, J. Kurths, and Z. Liu, Explosive synchronization in a general complex network, Phys. Rev. E **88**, 010802(R) (2013).
[29] H. J. Bi, X. Hu, S. Boccaletti, X.G. Wang, Y. Zou, Z.H. Liu, and S.G. Guan, Coexistence of Quantized, Time Dependent, Clusters in Globally Coupled Oscillators, Phys. Rev. Lett. **117**, 204101 (2016).
[30] H. Sakgauchi and Y. Kuramoto, A soluble active rotator model showing phase transitions via mutual entrainment, Prog. Theor. Phys. **86**, 576 (1986).
[31] M. A. Lohe, Synchronization control in networks with uniform and distributed phase lag, Automatica **54**, 114 (2015).
[32] E. Montbrió and D. Pazó, Shear diversity prevents collective synchronization, Phys. Rev. Lett. **106**, 254101 (2011).
[33] D. Pazó and E. Montbrió, The Kuramoto model with distributed shear, EPL **95**, 60007 (2011).
[34] Y. Kuramoto and D. Battogtokh, Coexistence of coherence and incoherence in nonlocally coupled phase oscillators, Nonlinear Phenom. Complex Syst. **5**, 380 (2002).
[35] D. Abrams and S. Strogatz, Chimera states for coupled oscillators, Phys. Rev. Lett. **93**, 174102 (2004).
[36] W. S. Lee, E. Ott, and T. M. Antonsen, Large coupled oscillator systems with heterogeneous interaction Delays, Phys. Rev. Lett. **103**, 044101 (2009).
[37] L. S. Tsimring, N. F. Rulkov, M. L. Larsen, and M. Gabbay, Repulsive synchronization in an array of phase oscillators, Phys. Rev. Lett. **95**, 014101 (2005).
[38] M. Li, X. G. Wang, and C. H. Lai, Evolution of functional subnetworks in complex systems, CHAOS **20**, 045114 (2010).
[39] P. Erdös and A. Rènyi, On random graphs. I, Publ. Math. **6**, 290 (1959).
[40] J. G. White, E. Southgate, J. N. Thompson, and S. Brenner, The structure of the nervous system of the nematode C. Elegans, Phil. Trans. R. Soc. London **314**, 1 (1986).
[41] W. K. Bickel and L. A. Marsch, Toward a behavioral economic understanding of drug dependence: delay discounting processes, Addiction **96**, 73 (2001).
[42] F. Varela, J.-P. Lachaux, E. Rodriguez, and J. Martinerie, The brainweb: Phase synchronization and large-scale integration, Nat. Rev. Neurosci. **2**, 229 (2001).
[43] L. Glass, Synchronization and rhythmic processes in physiology, Nature (London) **410**, 277 (2001).
[44] T. Nishikawa and A. E. Motter, Comparative analysis of existing models for power-grid synchronization, New J. Phys. **17**, 015012 (2015).
[45] F. Dörfler, M. Chertkov, and F. Bullo, Synchronization in complex oscillator networks and smart grids, Proc. Natl. Acad. Sci. U.S.A. **110**, 2005 (2013).
[46] P. J. Menck, J. Heitzig, J. Kurths, and H. J. Schellnhuber, How dead ends undermine power grid stability, Nat. Commun. **5**, 3969 (2014).
[47] V. Pappu, M. Carvalho, and P. Pardalos, *Optimization and security challenges in smart power grids* (Springer, 2013).
[48] Z. Qu, G. Hu, G. Yang, and G. Qin, Phase effect in taming nonautonomous chaos by weak harmonic perturbations, Phys. Rev. Lett. **74**, 1736 (1995).